(Received 9 August 2023, Accepted 10 November 2023, Scheduled 19 November 2023)

Modification of Fast Inverse Laplace Transform for Transient Response Analyses

Koki Watanabe*

Fukuoka Institute of Technology, Japan

ABSTRACT: The fast inverse Laplace transform (FILT) proposed by Hosono is recently applied to various transient response problems in electromagnetics. The frequency-domain methods have been the mainstream of electromagnetic simulation for many years, and a lot of knowledge has been accumulated. The FILT makes it possible to utilize frequency-domain techniques to transient analyses, and it is expected to provide reliable transient response analyses. Since the evaluation points of the image function in the conventional FILT depend on the observation time, the scope of application is sometimes limited when evaluation of the image function takes a relatively long computation time. This paper modifies the FILT so that the evaluation points are independent of the observation time, and the number of image function evaluations is reduced.

1. INTRODUCTION

Broad band signals are often used in recent applications of electromagnetic waves, and the time-domain simulations are drawing more attention. The most famous technique for the time-domain simulation may be the finite difference time-domain (FDTD) method [1], and it is used in a wide variety of transient phenomena. FDTD arranges the calculation points of the field components on a staggered grid, and the differential operations in the Maxwell equations are approximated by finite differences. The obtained relations are rearranged in the form of an update relations for time, and the field components are sequentially calculated for each time step. The basic idea of FDTD method is simple, but its relatively heavy computational cost sometimes limits the scope of application.

On a different note, transient phenomenon in electrical circuits has often been analyzed by using the Laplace transform, which converts differential equations into algebraic equations. However, since the inverse transform is relatively difficult to calculate, the Laplace transform has been used only for problems where the image function can be expressed as a superposition of the functions listed in the Laplace transform table [2]. Several methods have been proposed to numerically compute the inverse Laplace transform [3], and the fast inverse Laplace transform (FILT) [4] is one of such methods. The FILT does not require an analytical expression of the image function to obtain the original function, but estimates the value of the original function at the observation time from the values of the image function at a finite number of evaluation points. This implies that numerical analyses can be used to evaluate the image function. The transform parameter s, which is introduced by the Laplace transform, is also understood as an extension of the frequency to a complex number space, and the frequency-domain simulation techniques can be applied in many cases to evaluate the image function. The frequency-domain approaches have a long history, and we have a vast store of knowledge. The FILT makes it possible to utilize these knowledges for the transient response analyses of electromagnetic fields.

The FILT has been combined with various frequency-domain techniques and applied to a lot of transient problems [5–10]. However, the evaluation points of the image function depend on the observation time, and it is undesirable for the problems, in which evaluation of the image function takes a relatively long computation time. This paper proposes a simple modification of the FILT to fix the evaluation points of the image function and shows some results of numerical experiments to validate the modification. In this paper, $\Re(z)$, $\Im(z)$, and $\arg(z)$ denote respectively the real part, imaginary part, and argument angle of a complex number z. The superscript asterisk indicates complex conjugate.

2. CONVENTIONAL FILT

This section shows outline of the conventional FILT to make the calculation techniques clear and define the notations used in the following sections.

Let $f(t)$ be a piecewise continuous function of a real argument t satisfying $|f(t)| = O(e^{\alpha t})$ $(t \to \infty)$ with a real constant α. Then, the Laplace transform converts $f(t)$ to an image function $\tilde{f}(s)$ of a complex variable s, which is formally defined by

$$\tilde{f}(s) = \int_0^\infty f(t)\, e^{-s\,t}\, \mathrm{d}t, \tag{1}$$

for $\Re(s) > \alpha$ [3]. The image function $\tilde{f}(s)$ has no singular point in $\Re(s) > \alpha$, and it is often thought as extending its domain to the entire s-plane by the analytic continuation. The

* Corresponding authors: Koki Watanabe (koki@fit.ac.jp).

inverse transform is given by the Bromwich integral as

$$u(t)\,f(t) = \frac{1}{i\,2\,\pi}\int_{\sigma-i\,\infty}^{\sigma+i\,\infty} \tilde{f}(s)\,e^{s\,t}\,\mathrm{d}s \tag{2}$$

where σ is a real constant that satisfies $\sigma > \alpha$, and $u(t)$ denotes the Heaviside unit step function.

The FILT replaces the exponential function appearing in Eq. (2) by

$$\chi(z,\sigma_0) = \frac{e^{\sigma_0}}{2\,\cosh(z-\sigma_0)} \tag{3}$$

where σ_0 is an appropriate positive constant. The function $\chi(z,\sigma_0)$ gives a good approximation of e^z for z satisfying $e^{\Re(z)} \ll e^{\sigma_0}$ and $e^{2\,\sigma_0 - z}$ for z satisfying $e^{\Re(z)} \gg e^{\sigma_0}$. If σ_0 is chosen so as to satisfy $e^{\sigma_0} \gg e^{\alpha}$, the inverse Laplace transform (2) is approximated as

$$u(t)\,f(t) \approx \frac{1}{i\,2\,\pi}\int_{\sigma-i\,\infty}^{\sigma+i\,\infty} \tilde{f}(s)\,\chi(s\,t,\sigma_0)\,\mathrm{d}s \tag{4}$$

for σ satisfying $\sigma > \alpha$ and $e^{\sigma} \ll e^{\sigma_0}$. The function $\chi(z,\sigma_0)$ is periodic in the imaginary direction with period $2\,\pi$ and has simple poles at

$$z_n = \sigma_0 + i\,\pi\left(n - \frac{1}{2}\right) \tag{5}$$

for $n \in \mathbb{Z}$, where $\mathbb{Z}$ stands for the set of integers. Then, $\chi(z,\sigma_0)$ is also expressed in the partial fractional series as

$$\chi(z,\sigma_0) = \frac{i\,e^{\sigma_0}}{2}\sum_{n\in\mathbb{Z}}\frac{(-1)^n}{z-z_n}. \tag{6}$$

Substituting Eq. (6) into Eq. (4) and applying the residue theorem to evaluate the integrals, we may obtain an approximate expression of the inverse Laplace transform in the following form:

$$\begin{aligned} u(t)\,f(t) &\approx \frac{e^{\sigma_0}}{4\,\pi\,t}\sum_{n\in\mathbb{Z}}(-1)^n\int_{\sigma-i\,\infty}^{\sigma+i\,\infty}\frac{\tilde{f}(s)}{s-\frac{z_n}{t}}\,\mathrm{d}s \\ &= \frac{e^{\sigma_0}}{i\,2\,t}\sum_{n\in\mathbb{Z}}(-1)^n\,\tilde{f}\left(\frac{z_n}{t}\right). \end{aligned} \tag{7}$$

If the original function $f(t)$ is real, the image function satisfies $\tilde{f}(s^*) = \tilde{f}(s)^*$. Using an equality: ${z_{-n+1}} = {z_n}^*$, the inverse Laplace transform approximately expresses the original function $f(t)$ as

$$u(t)\,f(t) \approx \frac{e^{\sigma_0}}{t}\sum_{n\in\mathbb{N}}(-1)^n\,\Im\left(\tilde{f}\left(\frac{z_n}{t}\right)\right) \tag{8}$$

where $\mathbb{N}$ stands for the set of natural numbers.

Since the series appearing in Eq. (8) seems to be alternating, it is expected that its convergence is accelerated by the Euler transform [11]. Applying the Euler transform, Eq. (8) is taken into the following series:

$$u(t)\,f(t) \approx \frac{e^{\sigma_0}}{t}\sum_{n\in\mathbb{N}}\sum_{k=0}^{n-1}\frac{(-1)^k}{(-2)^n}\binom{n-1}{k}\Im\left(\tilde{f}\left(\frac{z_{n-k}}{t}\right)\right), \tag{9}$$

which is expected to converge more rapidly. In actual computation, the infinite series should be replaced by a sum of finite terms, and the FILT is often used in the following form:

$$\begin{aligned} u(t)\,f(t) \approx \frac{e^{\sigma_0}}{t}\Bigg[&\sum_{n=1}^{N_1}(-1)^n\,\Im\left(\tilde{f}\left(\frac{z_n}{t}\right)\right) \\ &+(-1)^{N_1}\sum_{n=1}^{N_2}w_n^{(N_2)}\,\Im\left(\tilde{f}\left(\frac{z_{N_1+n}}{t}\right)\right)\Bigg]. \end{aligned} \tag{10}$$

The expression of Eq. (7) is used for the first N_1 terms, and the expression of Eq. (9) is used for the following N_2 terms. The weights for the second summation $w_n^{(N)}$ are derived as

$$w_n^{(N)} = \frac{(-1)^n}{2^N}\sum_{k=n}^{N}\binom{N}{k} \tag{11}$$

and their values are recurrently obtained by

$$w_n^{(N)} = \begin{cases} \left(-\frac{1}{2}\right)^N & : n = N \\ -w_{n+1}^{(N)} + \frac{(-1)^n}{2^N}\binom{N}{n} & : n \in [1, N-1] \end{cases} \tag{12}$$

in descending order.

3. MODIFICATION OF FILT

As shown in Eq. (10), the conventional FILT evaluates the image function at discrete points $\{z_n/t\}$, which depend on the observation time t. It is undesirable when a relatively long computation time is required to evaluate the image function. In this section, a simple idea is proposed to reduce this difficulty.

Let t_{ref} be a reference time. The inverse Laplace transform Eq. (2) can be rewritten as

$$u(t)\,f(t) = \frac{1}{i\,2\,\pi}\int_{\sigma-i\,\infty}^{\sigma+i\,\infty}\tilde{f}(s)\,e^{s(t-t_{\mathrm{ref}})}\,e^{s\,t_{\mathrm{ref}}}\,\mathrm{d}s. \tag{13}$$

Replacing $e^{s\,t_{\mathrm{ref}}}$ by $\chi(s\,t_{\mathrm{ref}},\sigma_0)$ and using the expression given in Eq. (6), we may obtain the following approximation:

$$u(t)\,f(t) \approx \frac{e^{\sigma_0}}{4\,\pi\,t_{\mathrm{ref}}}\sum_{n\in\mathbb{Z}}(-1)^n\int_{\sigma-i\,\infty}^{\sigma+i\,\infty}\frac{\tilde{f}(s)\,e^{s(t-t_{\mathrm{ref}})}}{s-s_n}\,\mathrm{d}s \tag{14}$$

where $s_n = z_n/t_{\mathrm{ref}}$ for $n \in \mathbb{Z}$ denote the poles of $\chi(s\,t_{\mathrm{ref}},\sigma_0)$. The residue theorem is applied to evaluate the integrals for the case $t < t_{\mathrm{ref}}$ and yields the following approximation:

$$u(t)\,f(t) \approx \frac{e^{\sigma_0}}{i\,2\,t_{\mathrm{ref}}}\sum_{n\in\mathbb{Z}}(-1)^n\,\tilde{f}(s_n)\,e^{s_n(t-t_{\mathrm{ref}})}. \tag{15}$$

If the time function $f(t)$ is real, Eq. (15) is rewritten as

$$u(t)\,f(t) \approx \frac{e^{\sigma_0}}{t_{\rm ref}} \sum_{n\in\mathbb{N}} (-1)^n\ \Im(\tilde{f}(s_n)\,e^{s_n(t-t_{\rm ref})}), \qquad (16)$$

and the actual computation may be performed by the following finite series:

$$u(t)\,f(t) \approx \frac{e^{\sigma_0}}{t_{\rm ref}} \left[\sum_{n=1}^{N_1} (-1)^n\ \Im(\tilde{f}(s_n)\,e^{-s_n(t_{\rm ref}-t)}) \right.$$
$$\left. + (-1)^{N_1} \sum_{n=1}^{N_2} w_n^{(N_2)}\ \Im(\tilde{f}(s_{N_1+n})\,e^{-s_{N_1+n}(t_{\rm ref}-t)}) \right] \qquad (17)$$

This formula includes the values of image function evaluated at the poles of $\chi(s\,t_{\rm ref},\sigma_0)$, and the evaluation points $\{s_n\}$ are independent of the observation time t if $t < t_{\rm ref}$.

4. NUMERICAL EXPERIMENTS

To validate the present formulation, this section shows the results of some numerical experiments on fundamental transient problems. The absolute difference between $e^{s\,t}$ and $\chi(s\,t,\sigma_0)$ is approximately given as $|e^{s\,t} - \chi(s\,t,\sigma_0)| \approx e^{3\,\Re(s)\,t - 2\,\sigma_0}$ for $e^{\Re(s)\,t} \ll e^{\sigma_0}$, and the theoretical limit of the accuracy of FILT is estimated as $O(e^{-2\,\sigma_0})$ for large e^{σ_0} [4]. In this section, $\sigma_0 = 7$ is used for the numerical experiments. Also, we sometimes write $N_1 = 0$ or $N_2 = 0$, which means that the first or second summation in Eqs. (10) and (17) disappears.

4.1. Step Response of RLC Series Circuit

First, we consider an electric circuit, in which a resistor R, an inductor L, and a capacitor C are connected in series as shown in Fig. 1. Let $u(t)$ be the Heaviside unit step function, and apply a voltage $e(t) = A\,u(t)$ to the circuit. If the initial current is supposed to be $i(t) = 0$ for $t \le 0$, the image function of the current through the circuit is given by

$$\tilde{i}(s) = \frac{A\,C}{L\,C\,s^2 + R\,C\,s + 1} = \frac{A}{L}\,\frac{1}{(s-p_1)\,(s-p_2)} \qquad (18)$$

where the poles are given by $p_1 = -\alpha + \sqrt{\alpha^2 - \beta^2}$ and $p_2 = -\alpha - \sqrt{\alpha^2 - \beta^2}$ with $\alpha = R/\,(2\,L)$ and $\beta = 1/\sqrt{L\,C}$. Applying the inverse Laplace transform to Eq. (18), the exact expression of the current can be calculated analytically as follows:

$$i(t) = \begin{cases} u(t)\,\dfrac{A\,e^{-\alpha\,t}\,\sinh(\sqrt{\alpha^2-\beta^2}\,t)}{L\,\sqrt{\alpha^2-\beta^2}} & : \alpha > \beta \\ u(t)\,\dfrac{A}{L}\,t\,e^{-\alpha\,t} & : \alpha = \beta \\ u(t)\,\dfrac{A\,e^{-\alpha\,t}\,\sin(\sqrt{\beta^2-\alpha^2}\,t)}{L\,\sqrt{\beta^2-\alpha^2}} & : \alpha < \beta \end{cases} . \qquad (19)$$

Figure 2 shows numerical results of the conventional and the modified FILTs for the transient responses of RLC series circuit with the circuit parameters: $A/L = 1$, $\alpha = R/\,(2\,L) = 1$, and $\beta = 1/\sqrt{L\,C} = 0.1,\ 1,\ 10$. Three values $\beta = 0.1,\ 1,\ 10$ make the circuit over-damped, critically damped, and under-damped states, respectively, and the poles of the image function $\tilde{i}(s)$ are located at $p_1 \approx -0.005$ and $p_2 \approx -1.995$ for $\beta = 0.1$, $p_1 = p_2 = -1$ for $\beta = 1$, and $p_1 \approx -1 + i\,3.873$ and $p_2 \approx -1 - i\,3.873$ for $\beta = 10$. Both of the conventional and modified FILTs are performed with $N_1 = 10$ and $N_2 = 15$, and the reference times for the modified FILT are chosen as $t_{\rm ref} = 1, 2, 3$. The exact currents obtained from Eq. (19) are also drawn in Fig. 2, but they are not visible due to overlap with the results of the conventional FILT. The modified FILT seems to give rough estimations for $t \lesssim 1.4\,t_{\rm ref}$, though it is of no use for $t > 1.4\,t_{\rm ref}$. In the formulation shown in the previous section, this modification is thought to be valid only for $t < t_{\rm ref}$, but the practical range seems to have some difference. To check accuracy in more detail, the absolute errors of the numerical results shown in Fig. 2 are plotted in Fig. 3. This figure shows that the absolute error also increases when the observation time t is somewhat smaller than $t_{\rm ref}$. The modified FILT provides almost the same accuracy as the conventional one for $|t - t_{\rm ref}| \lesssim 0.2\,t_{\rm ref}$, and this is not very different for any of the three states.

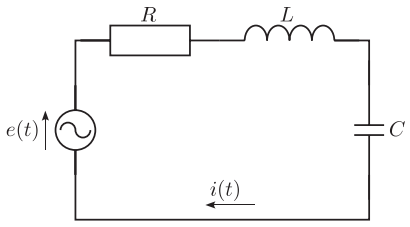

FIGURE 1. RLC series circuit.

Figure 4 shows the convergences of the mean absolute error (MAE) for $|t - t_{\rm ref}| \le 0.2\,t_{\rm ref}$. Let the division number be L, the time interval and evaluation points be given by $\Delta t = 0.2\,t_{\rm ref}/L$ and $t_l = t_{\rm ref} + l\,\Delta t$, respectively. Then, the MAE is here defined as

$$({\rm MAE}) = \frac{1}{2\,L+1} \sum_{l=-L}^{L} |i_{\rm FILT}(t_l) - i_{\rm exact}(t_l)| \qquad (20)$$

where $\{i_{\rm exact}(t_l)\}_{l=-L}^{L}$ are obtained from Eq. (19), and $\{i_{\rm FILT}(t_l)\}_{l=-L}^{L}$ are calculated by Eq. (10) or (17) with the truncation number $N = N_1 + N_2$. The values plotted in Fig. 4 are computed for $L = 50$ and $N_2 = N - N_1$ with various N_1, and the results of the modified and conventional FILTs are respectively denoted by the solid and dotted curves. Although the truncation number N_1 has to be chosen carefully especially for the under-damped state ($\alpha = 1$ and $\beta = 10$), the convergence acceleration by Euler transformation is very effective for the modified FILT as well as for the conventional FILT. From Fig. 4, we can see that the convergence of the modified FILT is not much worse than that of the conventional one. Considering the modified FILT requires only N values $\{\tilde{f}(s_n)\}_{n=1}^{N}$ to compute $f(t)$ in the time domain $0.8\,t_{\rm ref} \lesssim t \lesssim 1.2\,t_{\rm ref}$, we may understand that the present modification contributes sufficiently to reducing the number of evaluations of the image function.

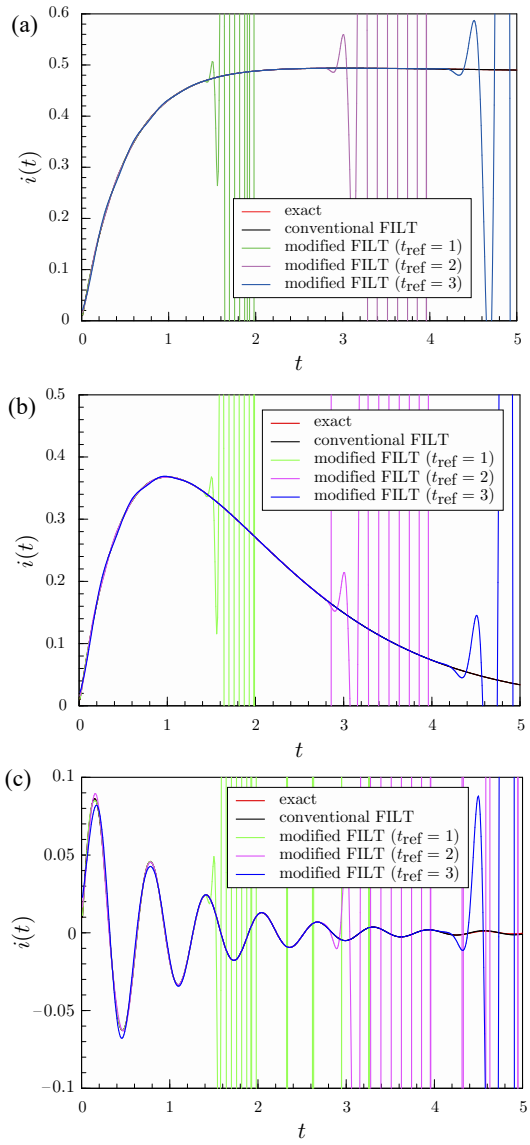

FIGURE 2. Transient currents through the RLC series circuit. (a) $\alpha = 1$ and $\beta = 0.1$. (b) $\alpha = 1$ and $\beta = 1$. (c) $\alpha = 1$ and $\beta = 10$.

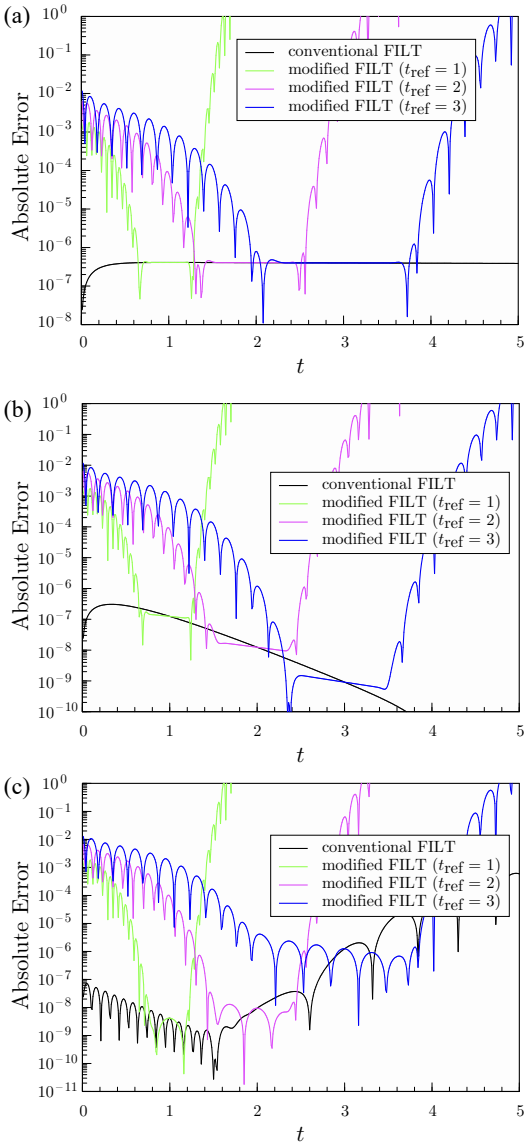

FIGURE 3. Absolute errors of the transient currents obtained by the FILT. (a) $\alpha = 1$ and $\beta = 0.1$. (b) $\alpha = 1$ and $\beta = 1$. (c) $\alpha = 1$ and $\beta = 10$.

4.2. Electromagnetic Pulse Response of Dielectric Circular Cylinder

Next, we consider a transient problem of the pulse electromagnetic-wave scattering by a dielectric circular cylinder. Fig. 5 shows the geometry under consideration. An infinitely long circular cylinder of radius a is concentric with the z-axis, and it is made with a homogeneous, isotropic, and non-dispersive medium described by permittivity ε_c and permeability μ_c. The surrounding region is filled by a lossless, homogeneous, isotropic, and non-dispersive medium with permittivity ε_s and permeability μ_s. The speed of light and characteristic impedance in each medium are respectively denoted by $c_r = 1/\sqrt{\varepsilon_r \mu_r}$ and $\zeta_r = \sqrt{\mu_r/\varepsilon_r}$ for $r = c, s$. The incident fields are supposed to be a Gaussian-type pulse plane-wave propagating in the $-x$-direction, and the pulse center at $t = 0$ is denoted by $x = x_p$. Since the electromagnetic fields are uniform in the z-direction, the problem becomes two-dimensional, and two fundamental polarizations are expressed by TM and TE, in which the magnetic and electric fields are respectively perpendicular to the z-axis. The z-component of the electric field for the TM-polarization and the z-component of the magnetic field for the TE-polarization are denoted by $\psi(x, y, t)$, and relations for both polarizations are simultaneously shown.

Since the Gaussian function has non-zero values on the entire domain, it is not very tractable for defining incident waves in the transient analyses based on the Laplace transform. Therefore, the incident field is here defined by pseudo-Gaussian pulse [12] as

$$\psi^{(i)}(x,t) = \psi_0\, p_{2M}\left(t; \frac{x_p - x}{c_s}, t_\sigma\right) \tag{21}$$

where ψ_0 is the amplitude; $p_{2M}(t; t_\mu, t_\sigma)$ denotes the $(2M)$th-order pseudo-Gaussian function ($M \in \mathbb{N}$); and t_σ determines

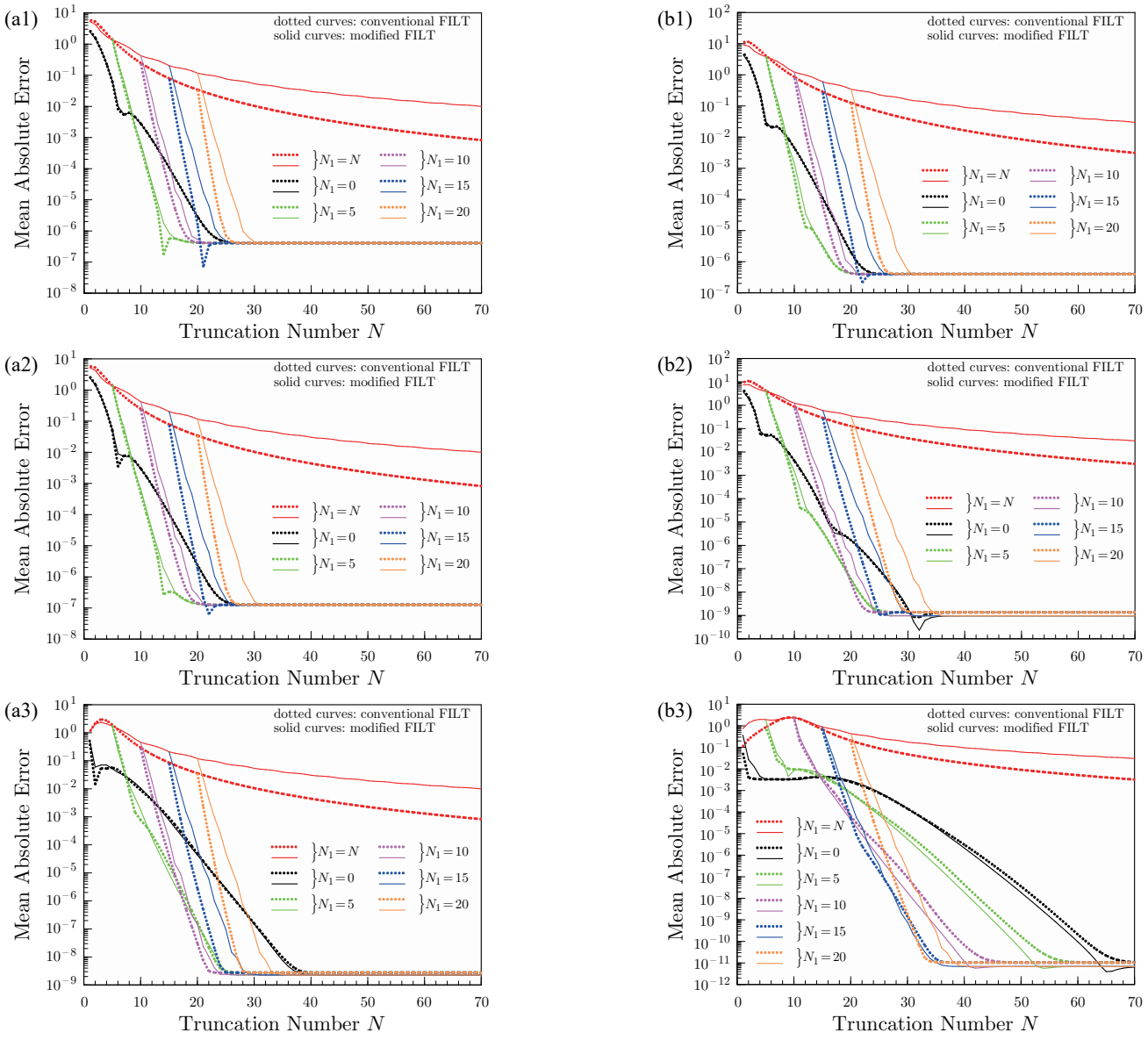

FIGURE 4. Convergence characteristics for the step response of RLC series circuit. (a1) $t_{\text{ref}} = 1$ ($\alpha = 1$ and $\beta = 0.1$). (a2) $t_{\text{ref}} = 1$ ($\alpha = 1$ and $\beta = 1$). (a3) $t_{\text{ref}} = 1$ ($\alpha = 1$ and $\beta = 10$). (b1) $t_{\text{ref}} = 3$ ($\alpha = 1$ and $\beta = 0.1$). (b2) $t_{\text{ref}} = 3$ ($\alpha = 1$ and $\beta = 1$). (b3) $t_{\text{ref}} = 3$ ($\alpha = 1$ and $\beta = 10$).

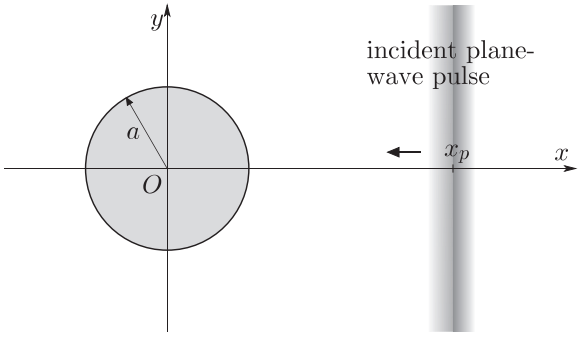

FIGURE 5. Pulse plane-wave scattering by dielectric circular cylinder.

the pulse width in the time-domain. The pseudo-Gaussian function $p_{2M}(t; t_\mu, t_\sigma)$ is defined by

$$p_{2M}(t; t_\mu, t_\sigma) = \begin{cases} \cos^{2M}\left(\frac{\pi}{2\,t_w}\,(t - t_\mu)\right) : & |t - t_\mu| \le t_w \\ 0 : & |t - t_\mu| > t_w \end{cases} \tag{22}$$

with $t_w = \pi\sqrt{M/2}\,t_\sigma$, and gives a good approximation of $\exp[-(t - t_\mu)^2 / (2\,t_\sigma{}^2)]$ for large M. When $t_\mu > t_w$ is satisfied, the image function of $p_{2M}(t; t_\mu, t_\sigma)$ is derived as

$$\tilde{p}_{2M}(s; t_\mu, t_\sigma) = 2^{-2\,M+1}\, e^{-t_\mu\, s}\, \sinh(t_w\, s) \left[\binom{2\,M}{M} \frac{1}{s} + \sum_{k=1}^{M} \binom{2\,M}{M-k} \frac{2\,(-1)^k\, s}{s^2 + \left(\frac{\pi\, k}{t_w}\right)^2} \right]. \tag{23}$$

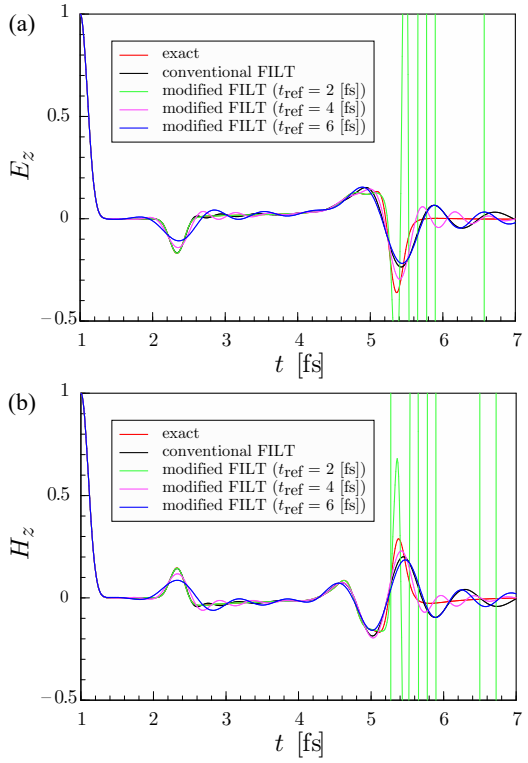

FIGURE 6. Transient field response of pulse plane-wave scattering by a dielectric circular cylinder. (a) TM-polarization. (b) TE-polarization.

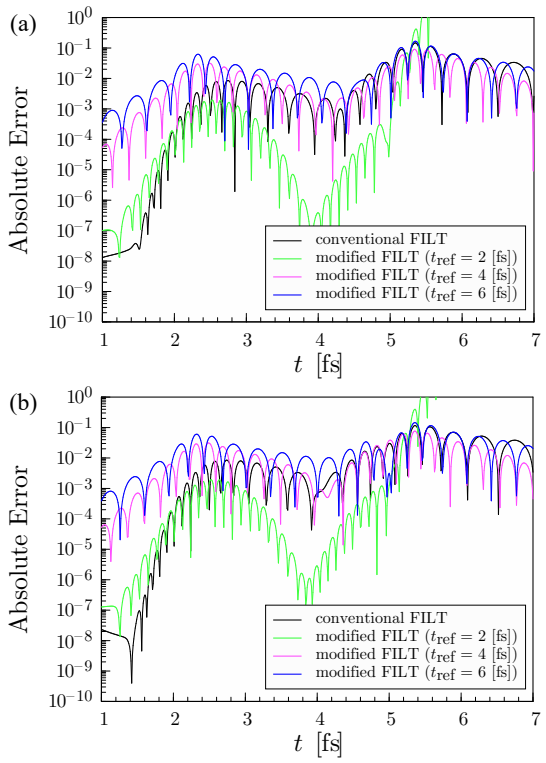

FIGURE 7. Absolute errors of transient field response computed with $\sigma_0 = 7$, $N_1 = 10$, and $N_2 = 15$. (a) TM-polarization. (b) TE-polarization.

Then the image function of the incident field in $x < x_p - c_s\, t_w$ is given by

$$\tilde{\psi}^{(i)}(x,s) = \psi_0\, \tilde{p}_{2M}\left(s; \frac{x_p}{c_s}, t_\sigma\right) e^{\frac{s}{c_s}\, x}. \tag{24}$$

Here, we also use the cylindrical coordinate system O-$\rho\phi z$, which is related to the original coordinate system O-xyz by transformation equations: $\rho = \sqrt{x^2 + y^2}$ and $\phi = \arg(x + i\, y)$. If the initial position of the pulse center satisfies $x_p > a + c_s\, t_w$, the incident field illuminates the cylinders from outside, and the its image function can be expressed near the cylinder as

$$\tilde{\psi}^{(i)}(\rho,\phi,s) = \psi_0\, \tilde{p}_{2M}\left(s; \frac{x_p}{c_s}, t_\sigma\right)\left(I_0\left(\frac{\rho\, s}{c_s}\right) + 2\sum_{q\in\mathbb{N}} I_q\left(\frac{\rho\, s}{c_s}\right)\cos(q\,\phi)\right) \tag{25}$$

where $I_q(\cdot)$ denotes the qth-order modified Bessel function of the first kind. Considering the boundary conditions at the cylinder surface $\rho = a$, the image function of the scattered field for $\rho > a$ is expressed in the cylindrical-wave expansion as

$$\tilde{\psi}^{(s)}(\rho,\phi,s) = \psi_0\, \tilde{p}_{2M}\left(s; \frac{x_p}{c_s}, t_\sigma\right)$$

$$\left(t_0(s)\, K_0\left(\frac{\rho\, s}{c_s}\right) + 2\sum_{q\in\mathbb{N}} t_q(s)\, K_q\left(\frac{\rho\, s}{c_s}\right)\cos(q\,\phi)\right) \tag{26}$$

where $K_q(\cdot)$ denotes the qth-order modified Bessel function of the second kind, and the expansion coefficients $\{t_q\}$ are given by

$$t_q(s) = \begin{cases} -\dfrac{\zeta_s\, I_q(\frac{a}{c_s}\, s)\, I_q'(\frac{a}{c_c}\, s) - \zeta_c\, I_q'(\frac{a}{c_s}\, s)\, I_q(\frac{a}{c_c}\, s)}{\zeta_s\, K_q(\frac{a}{c_s}\, s)\, I_q'(\frac{a}{c_c}\, s) - \zeta_c\, K_q'(\frac{a}{c_s}\, s)\, I_q(\frac{a}{c_c}\, s)} & : \text{TM-pol.} \\ -\dfrac{\zeta_s\, I_q'(\frac{a}{c_s}\, s)\, I_q(\frac{a}{c_c}\, s) - \zeta_c\, I_q(\frac{a}{c_s}\, s)\, I_q'(\frac{a}{c_c}\, s)}{\zeta_s\, K_q'(\frac{a}{c_s}\, s)\, I_q(\frac{a}{c_c}\, s) - \zeta_c\, K_q(\frac{a}{c_s}\, s)\, I_q'(\frac{a}{c_c}\, s)} & : \text{TE-pol.} \end{cases}. \tag{27}$$

Alternatively, the image function of the total field inside the cylinder ($\rho < a$) is expressed as

$$\tilde{\psi}(\rho,\phi,s) = \psi_0\, \tilde{p}_{2M}\left(s; \frac{x_p}{c_s}, t_\sigma\right)$$

$$\left(u_0(s) I_0\left(\frac{\rho s}{c_c}\right) + 2\sum_{q\in\mathbb{N}} u_q(s) I_q\left(\frac{\rho s}{c_c}\right)\cos(q\phi)\right) \tag{28}$$

with the expansion coefficients:

$$u_q(s) = \frac{I_q(\frac{a}{c_s}\, s) + K_q(\frac{a}{c_s}\, s)\, t_q(s)}{I_q(\frac{a}{c_c}\, s)}. \tag{29}$$

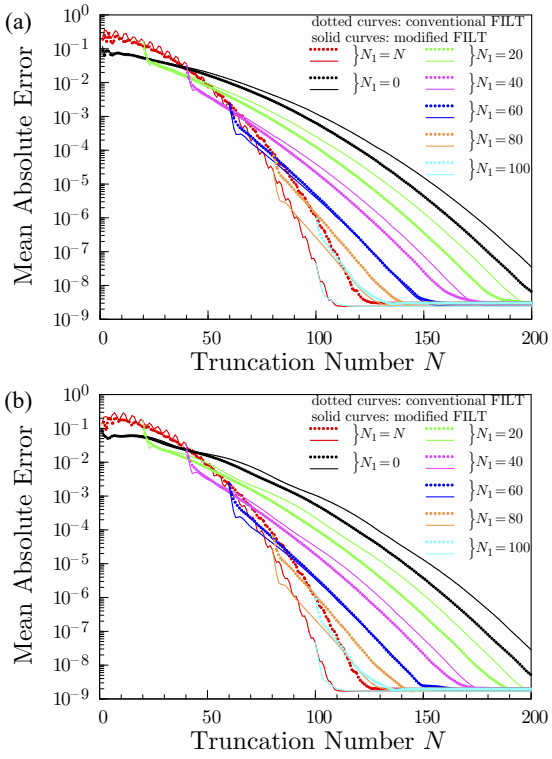

FIGURE 8. Convergence characteristics for the pulse response. (a) TM-polarization. (b) TE-polarization.

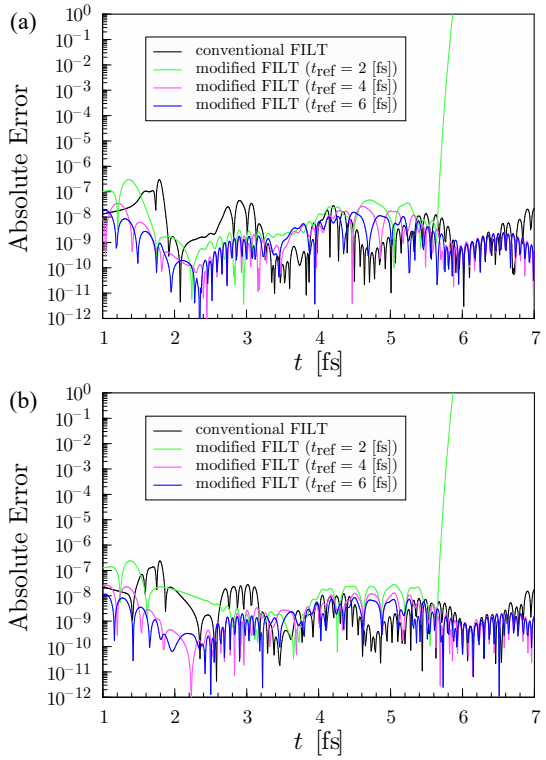

FIGURE 9. Absolute errors of transient field response computed with $\sigma_0 = 7$, $N_1 = 120$, and $N_2 = 0$. (a) TM-polarization. (b) TE-polarization.

Let us choose the structural parameters for numerical calculation as follows: $\varepsilon_s = \varepsilon_0$, $\varepsilon_c = 5\,\varepsilon_0$, $\mu_s = \mu_c = \mu_0$, and $a = 100\,\text{nm}$. Also, the parameters for the incident pulse plane-wave are chosen as $M = 18$, $x_p = 600\,\text{nm}$, $t_\sigma = 0.1\,\text{fs}$, and $\psi_0 = 1$. Fig. 6 shows the numerical results of the z-components of the fields at $(x, y) = (0.5\,x_p, 0)$. The exact solution to this problem has not been found, and the "exact" values drawn by the red curves in Fig. 6 are calculated by the extrapolation technique [13] after performing calculations by the conventional FILT with different values of σ_0, the truncation number for the FILT: $N = N_1 + N_2$, and the truncation number for the infinite sum in Eq. (26). The absolute errors of the "exact" values are estimated to be less than 10^{-8}. In this subsection, the results of the conventional and modified FILTs are obtained by truncating the infinite sums in Eqs. (26) and (28) at $q = 20$, and the error due to this truncation is considered sufficiently small. The parameters for the FILT are $N_1 = 10$ and $N_2 = 15$, and the reference times for the modified FILT are chosen as $t_{\rm ref} = 2, 4, 6\,\text{fs}$. Rough trends are obtained except for the modified FILT with $t_{\rm ref} = 2\,\text{fs}$ in $t > 5.2\,\text{fs}$. Fig. 7 shows the absolute errors of the numerical results in Fig. 6. It is observed that the modified FILT provides almost the same accuracy as the conventional one near the reference time $t_{\rm ref}$, but the errors are relatively large under this calculation condition.

Figure 8 shows convergence characteristics of the MAE for $|t - t_{\rm ref}| \le 0.2\,t_{\rm ref}$, where "$i$" appearing in Eq. (20) is replaced by "ψ". The values are computed for $t_{\rm ref} = 6\,\text{fs}$, $L = 50$, and $N_2 = N - N_1$ with various N_1, and the results of the modified and conventional FILTs are respectively shown by the solid and dotted curves. The convergence acceleration by introducing the Euler transform seems to have only a limited effect, and the convergence becomes rather slow after showing a slight improvement. It is observed that there are no significant differences in the convergences of the conventional and modified FILTs.

Figure 9 shows the results of the same calculation as Fig. 7 but with $N_1 = 120$ and $N_2 = 0$. The convergence characteristics shown in Fig. 8 are of the MAE calculated by the values for $4.8\,\text{fs} \le t \le 7.2\,\text{fs}$, but high-precision calculations for $1\,\text{fs} \le t < 4.8\,\text{fs}$ can also be achieved. In Section 4.1, the modified FILT provides almost the same accuracy as the conventional one only for time domain: $|t - t_{\rm ref}| \lesssim 0.2\,t_{\rm ref}$. However, the modified FILT provides here almost the same accuracy as the conventional one in much wider time domain, and the value of $\psi(0.5\,x_p, 0, t)$ at any time in the domain $1\,\text{fs} \le t \le 7\,\text{fs}$ may be accurately estimated from 120 values of the image function $\{\tilde{\psi}^{(s)}(0.5\,x_p, 0, z_n/t_{\rm ref})\}_{n=1}^{120}$ if the reference time is chosen to $t_{\rm ref} = 4\,\text{fs}$ or $6\,\text{fs}$.

The E_z-component distributions of the TM-polarized fields near the cylinder are computed at three observation times $t = 2, 4.5, 7\,\text{fs}$ and shown in Fig. 10. The three figures on the left are the results of the modified FILT computed with $N_1 = 120$, $N_2 = 0$, $t_{\rm ref} = 6\,\text{fs}$, and the image function is evaluated at the same points $\{z_n/t_{\rm ref}\}_{n=1}^{N}$. On the other hand, the three figures on the right are the results of the conventional FILT,

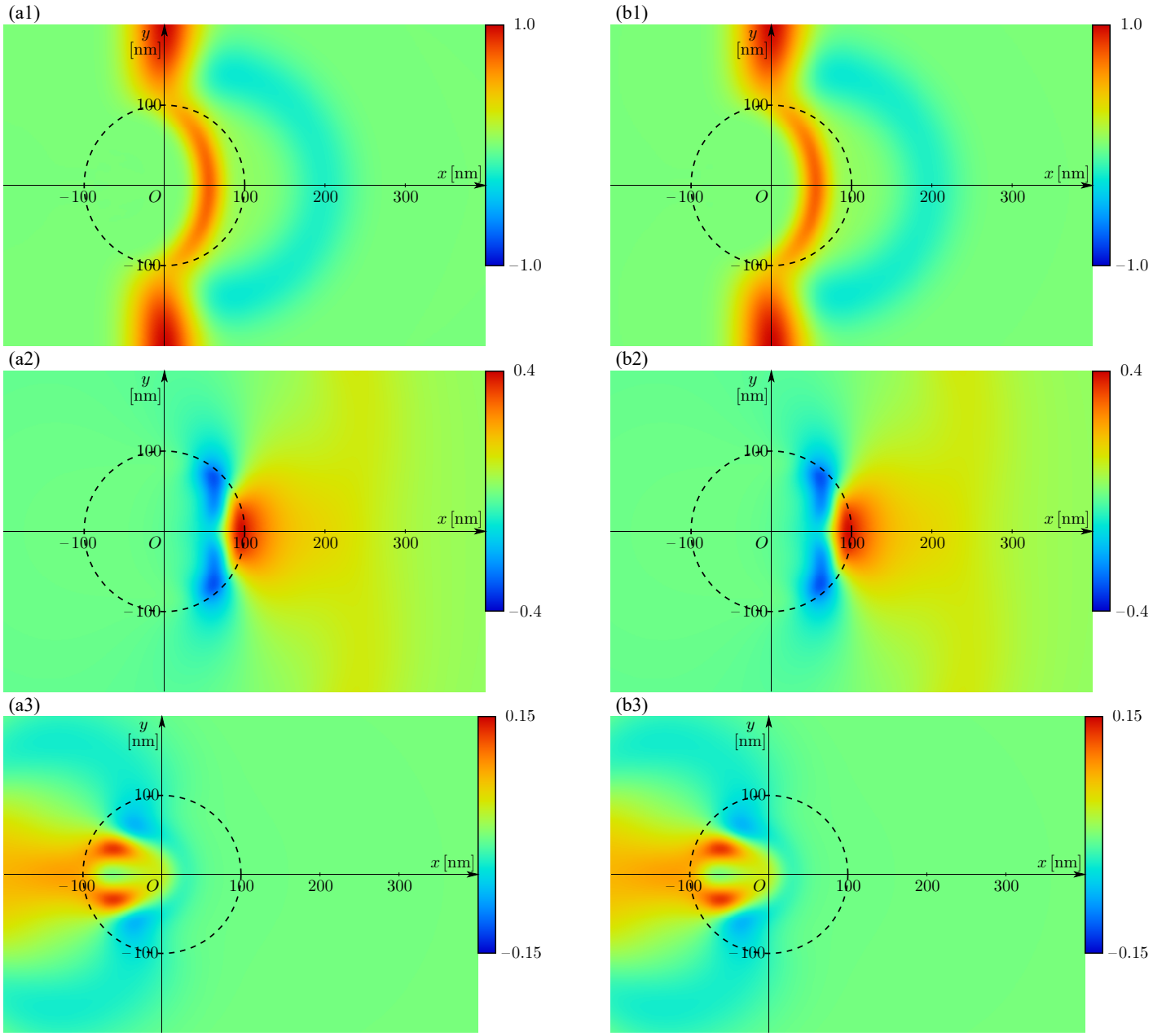

FIGURE 10. The E_z-component of the TM-polarized fields computed by the modified and the conventional FILT for $t = 2, 4.5, 7$ fs. (a1) modified FILT ($t = 2$ fs). (a2) modified FILT ($t = 4.5$ fs). (a3) modified FILT ($t = 7$ fs). (b1) conventional FILT ($t = 2$ fs). (b2) conventional FILT ($t = 4.5$ fs). (b3) conventional FILT ($t = 7$ fs).

and the evaluation points of the image function depend on the observation time. The truncation numbers used for Fig. 10 are determined by the convergence test at an observation point $(x, y) = (0.5\,x_p, 0)$, but these figures show no difference between the results computed by the modified and conventional FILTs. Each figure in Fig. 10 uses the computed results at $301 \times 201 = 60501$ equally spaced points, and the maximum absolute difference between the results of the modified and conventional FILTs is 2.6×10^{-7} for $t = 2$ fs, 8.9×10^{-8} for $t = 4.5$ fs, and 2.1×10^{-7} for $t = 7$ fs. This implies that, at least near the cylinder, the modified FILT with a fixed set of evaluation points for the image function can perform calculations as accurately as the conventional FILT over a wide time domain.

5. CONCLUDING REMARKS

This paper considers the FILT used for transient response analyses. The conventional formulation of FILT needs to evaluate the image function for each observation time, and it is sometimes difficult to apply to problems that require a relatively long computation time to evaluate the image function. The present paper proposed a simple modification to resolve this difficulty, and the present modification was validated by some numerical experiments. The numerical results reveal that the modi-

fied FILT without changing the evaluation points of the image functions can provide almost the same accuracy as the conventional one in a certain time domain. Although further theoretical researches are needed to predict the effective time domain and truncation numbers, it was found that the modified method presented in this paper is sufficiently effective in reducing the number of image function evaluations.

REFERENCES

[1] Taflove, A. and S. C. Hagness, *Computational Electrodynamics: The Finite-Difference Time-Domain Method*, Artech house, Norwood, 2005.

[2] Oberhettinger, F. and L. Badii, *Tables of Laplace Transforms*, Springer-Verlag, Berlin, 1973.

[3] Cohen, A. M., *Numerical Methods for Laplace Transform Inversion*, Springer, New York, 2010.

[4] Hosono, T., "Numerical inversion of Laplace transform and some applications to wave optics," *Radio Sci.*, Vol. 16, No. 6, 1015–1019, 1981.

[5] Hosono, H., "Transient responses of electromagnetic waves scattered by a circular cylinder with longitudinal slots - The case of back scattering by a cylinder with a slot in the forward direction," *IEICE Trans. Electron.*, Vol. E74-C, No. 9, 2864–2869, 1991.

[6] Kishimoto, S., T. Okada, S. Ohnuki, Y. Ashizawa, and K. Nakagawa "Efficient analysis of electromagnetic fields for designing nanoscale antennas by using a boundary integral equation method with fast inverse Laplace transform," *Progress In Electromagnetics Research*, Vol. 146, 155–165, 2014.

[7] Ohnuki, S., Y. Kitaoka, and T. Takeuchi, "Time-domain solver for 3D electromagnetic problems using the method of moments and the fast inverse Laplace transform," *IEICE Trans. Electron.*, Vol. E99-C, No. 7, 797–800, 2016.

[8] Ozaki, R. and T. Yamasaki, "Analysis of pulse responses from conducting strips with dispersion medium sandwiched air layer," *IEICE Electron. Express*, Vol. 15, No. 6, 1–6, 2018.

[9] Ohnuki, S., "Time-domain analysis of electromagnetic waves using fast inverse Laplace transform," *Trans. IEICE Japan*, Vol. J103-C, No. 4, 203–210, 2020 (in Japanese).

[10] Kishimoto, S., S. Nishino, and S. Ohnuki, "Novel computational technique for time-dependent heat transfer analysis using fast inverse Laplace transform," *Progress In Electromagnetics Research M*, Vol. 99, 45–55, 2021.

[11] Abramowitz, M. and I. Stegun (eds.), *Handbook of Mathematical Functions with Formulas, Graphs, and Mathematical Tables*, Dover, New York, 1972.

[12] Hosono, H. and T. Hosono, "Highly anomalous propagation of pseudo-Gaussian pulse," *IEICE Trans. Electron.*, Vol. E90-C, No. 2, 224–230, 2007.

[13] Yamasaki, T., K. Isono, and T. Hinata, "Analysis of electromagnetic fields in inhomogeneous media by Fourier series expansion methods — The case of a dielectric constant mixed a positive and negative regions," *IEICE Trans. Electron.*, Vol. E88-C, No. 12, 2216–2222, 2005.